Video Article

Investigating the Spreading and Toxicity of Prion-like Proteins Using the Metazoan Model Organism *C. elegans*

Carmen I. Nussbaum-Krammer[1], Mário F. Neto[1], Renée M. Brielmann[1], Jesper S. Pedersen[1], Richard I. Morimoto[1]

[1]Department of Molecular Biosciences, Rice Institute for Biomedical Research, Northwestern University

Correspondence to: Carmen I. Nussbaum-Krammer at c.nussbaum@zmbh.uni-heidelberg.de

URL: http://www.jove.com/video/52321
DOI: doi:10.3791/52321

Keywords: Cellular Biology, Issue 95, *Caenorhabditis elegans*, neurodegenerative diseases, protein misfolding diseases, prion-like spreading, cell-to-cell transmission, protein aggregation, non-cell autonomous toxicity, proteostasis

Date Published: 1/8/2015

Citation: Nussbaum-Krammer, C.I., Neto, M.F., Brielmann, R.M., Pedersen, J.S., Morimoto, R.I. Investigating the Spreading and Toxicity of Prion-like Proteins Using the Metazoan Model Organism *C. elegans*. *J. Vis. Exp.* (95), e52321, doi:10.3791/52321 (2015).

Abstract

Prions are unconventional self-propagating proteinaceous particles, devoid of any coding nucleic acid. These proteinaceous seeds serve as templates for the conversion and replication of their benign cellular isoform. Accumulating evidence suggests that many protein aggregates can act as self-propagating templates and corrupt the folding of cognate proteins. Although aggregates can be functional under certain circumstances, this process often leads to the disruption of the cellular protein homeostasis (proteostasis), eventually leading to devastating diseases such as Alzheimer's disease (AD), Parkinson's disease (PD), Amyotrophic lateral sclerosis (ALS), or transmissible spongiform encephalopathies (TSEs). The exact mechanisms of prion propagation and cell-to-cell spreading of protein aggregates are still subjects of intense investigation. To further this knowledge, recently a new metazoan model in *Caenorhabditis elegans*, for expression of the prion domain of the cytosolic yeast prion protein Sup35 has been established. This prion model offers several advantages, as it allows direct monitoring of the fluorescently tagged prion domain in living animals and ease of genetic approaches. Described here are methods to study prion-like behavior of protein aggregates and to identify modifiers of prion-induced toxicity using *C. elegans*.

Video Link

The video component of this article can be found at http://www.jove.com/video/52321/

Introduction

Many neurodegenerative diseases, including Alzheimer's disease (AD), Parkinson's disease (PD), Amyotrophic lateral sclerosis (ALS), and transmissible spongiform encephalopathies (TSEs), are associated with aggregation-prone proteins and are hence collectively known as protein misfolding disorders (PMDs). TSEs or prion diseases constitute a unique class of PMDs in that they can be infectious in both humans and animals[1]. At the molecular level, prions replicate by recruiting and converting monomeric α-helix-rich host-encoded cellular PrP (PrP^{C}) into the pathological β-sheet-rich PrP^{Sc} conformation[2,3]. Self-propagating protein aggregates have been also identified in fungi, which share important characteristics with mammalian prions[4,5]. Additionally, mammalian prions are capable of moving from cell-to-cell and infect naïve cells[6,7].

While PMDs other than TSEs are not infectious, they share a common pathogenic principle with prion diseases[8,9]. Although the proteins linked to each of the PMDs are not related in structure or function, they all form aggregates via a crystallization-like process called nucleated or seeded polymerization; moreover proteinaceous seeds grow by recruiting their soluble isoforms[2,10,11]. The efficiency to self-propagate varies *in vivo*, depending on the intrinsic properties of the protein, which together with additional cellular factors such as molecular chaperones ultimately determine rates of aggregate nucleation, seeding, fragmentation and spreading[12-15]. Hence, there must exist a fine balance among these factors that allows efficient propagation of protein aggregation. This might also explain why only some amyloidogenic aggregates harbor the characteristics of a prion, and thus not all PMDs are infectious. Prions seem to represent 'top-performers' of a wide spectrum of self-replicating proteinaceous aggregates, which makes them a powerful tool to study PMDs[8,13].

Intriguingly, the toxicity associated with disease-related aggregates often has a non cell autonomous component[16,17]. This means that they affect neighboring cells that do not express the corresponding gene, in contrast to a strictly cell autonomous effect, which implies that only the cells expressing the gene exhibit the specific phenotype. This was compellingly demonstrated by tissue-specific expression or knock down of the respective proteins in numerous models of neurodegenerative diseases[18-26]. Various mechanisms have been suggested as a basis for this non-cell autonomous toxicity in PMDs, including diminished nutrient supply, imbalance in neuronal signaling, glutamate excitotoxicity, and neuroinflammation[16,27,28]. In addition, a prion-like movement of disease-linked aggregates between cells might contribute to this aspect[29,30]. Increasing evidence suggests that protein inclusions other than prions can transmit from cell-to-cell, which may explain the characteristic spreading of pathology observed in many PMDs[30-36]. However, it has yet to be determined whether there is a clear causal link between intercellular movement of disease proteins and the toxic effect on neighboring cells. Therefore, a better understanding of the cellular pathways that underlie cell-to-cell transmission and non cell autonomous toxicity is necessary and essential for the development of novel therapeutics.

However, many aspects of prion-like spreading and cellular factors that influence cell-to-cell transmission of misfolded proteins in metazoans are not well understood, in particular at the organismal level.

The nematode *Caenorhabditis elegans* has several advantages that provide the potential to discover new facets of prion-like spreading in metazoans[17]. It is transparent, allowing for *in vivo* tracking of fluorescently tagged proteins in the living organism. Furthermore, many cellular and physiological processes affected by disease are conserved from worms to human, and *C. elegans* is also amenable to a wide variety of genetic manipulations and molecular and biochemical analyses[37-39]. Exactly 959 somatic cells make up the adult hermaphrodite with a simple body plan that still has several distinct tissue types, including muscle, neurons and intestine.

To establish a new prion model in *C. elegans,* we chose to exogenously express the well characterized glutamine/asparagine (Q/N)-rich prion domain NM of the cytosolic yeast prion protein Sup35, since there are no known endogenous prion proteins in worms[4,40]. Yeast prions have been invaluable in elucidating basic mechanisms of prion replication[41-44]. Furthermore, NM is the first cytosolic prion-like protein that has been shown to recapitulate the full life cycle of a prion in mammalian cell culture[45,46]. Likewise, when expressed in *C. elegans*, the Sup35 prion domain adopted remarkably well to the different requirements for propagation in metazoan cells compared to yeast cells and exhibited key features of prion biology[40]. NM aggregation was associated with a profound toxic phenotype, including the disruption of mitochondrial integrity and appearance of various autophagy related vesicles on the cellular level, as well as embryonic and larval arrest, developmental delay, and a widespread disturbance of the protein folding environment on the organismal level. Strikingly, the prion domain exhibits cell autonomous and non cell autonomous toxicity, affecting neighboring tissues in which the transgene was not expressed. Furthermore, the vesicular transport of the prion domain within and between cells is monitored real time *in vivo*[40].

Here we describe how to examine prion-like dissemination in *C. elegans*. We will explain how to monitor the intra- and intercellular transport of vesicles containing the prion domain using time-lapse fluorescence microscopy. We will emphasize the use of tissue-specific folding sensors and ubiquitously expressed stress reporters to evaluate cell autonomous and non cell autonomous effects on cellular fitness. Finally, we will describe the procedure of a recently performed genome wide RNA interference (RNAi) screen to identify new modifiers of prion-induced toxicity. In combination, these methods can help to tease apart genetic pathways involved in the intercellular movement of proteins and their non cell autonomous toxicity.

Protocol

1. Monitoring Transcellular Spreading of Prion-like Proteins By *In Vivo* Time-lapse Imaging

NOTE: Grow *C. elegans* wild-type (WT) (N2) and transgenic lines according to standard methods and carefully control the cultivation temperature[47].

1. Generate transgenic lines of *C. elegans* expressing the prion-like protein, tagged with monomeric red fluorescent protein (mRFP). Watch this video that demonstrates how to use microinjection[48]. For further details and methods describing how to integrate these extrachromosomal lines, see[49].
2. Prepare synchronized populations by egg laying or bleaching according to standard methods[50].
    1. Synchronization by egg laying
        1. Transfer 10 - 20 gravid adults on a plate and let them lay eggs for 1 - 2 hr. Remove adults from the plate and let the progeny grow until the desired age.
    2. Synchronization by bleaching
        1. Collect an unsynchronized population of gravid adults and bleach them with alkaline hypochlorite solution (250 mM NaOH and 1:4 (v/v) dilution of commercial bleach in H_2O). Wash the eggs twice (218 x g for 1 min) with M9 buffer[47] (21 mM$Na_2HPO_4{\cdot}7H_2O$, 22 mMKH_2PO_4, 86 mMNaCl, 1 mM$MgSO_4{\cdot}7H_2O$, add dH_2O up to 1 L).
        2. Allow them to hatch in M9 buffer with gentle agitation O/N at 20 °C. Worm development will arrest at the L1 stage in the absence of a food source, leaving a synchronized population. Transfer L1s onto fresh Nematode Growth Media (NGM) plates seeded with OP50 *E. coli* bacteria and let the progeny develop until the desired age[47].
3. Prepare 2% agarose pads (in H_2O) on a microscope slide as described[50].
    1. Prepare two microscope slides with labeling tape placed over their entire length to be used as spacers. Place a third microscope slide between them.
    2. Dissolve 2% agarose in H_2O and pipette one drop onto the clean slide.
    3. Place a fourth slide perpendicular to the three other slides on top of the agar drop. Gently press it down to flatten the pad to the same thickness as the labeling tape.
    4. Let it dry for 1 min before removing the spacers and gently pulling the slides apart. The agar pad will stick to one of them.
4. Pipette ~10 µl anesthetic (2 mM levamisole in M9 buffer) to the pad and transfer ~10 animals using a platinum wire pick. Cover with a cover slip (~22 x 22 mm) and take images within 1 hr.
5. Alternatively, to acquire movies over a longer period of time or to further reduce the possibility of any movement of the animals, use a combination of anesthetic and bead immobilization[51].
    1. Prepare 10% agarose pads (in M9 buffer) as described[51] and add worms to 3 µl nanosphere size standards solution (polystyrene beads, 100 nm) plus 3 µl anesthetic (4 mM levamisole in M9 buffer). Cover gently with a cover slip. To avoid desiccation, seal the cover slip with VALAP (mixture of equal amounts of Vaseline, lanolin, and paraffin wax).
6. Image immobilized worms using a confocal microscope.

NOTE: Results are obtained using a Spinning Disc AF Confocal Microscope equipped with an EM-CCD camera and a Microscopy Automation & Image Analysis Software such as MetaMorph and outline the specifics below, but other comparable confocal imaging systems can also be used.

1. Use the 63X or 100X/1.4NA oil objective and place the microscope slide containing worms into the microscope slide holder.
2. Open the software. Adjust laser power and filters for mRFP imaging. Use the 561 nm laser at 10% power and emission filter >600 nm.
3. Open “MultiDimensional Acquisition”. Under the “Main” tab, check the boxes for “Timelapse” and “Run Journals” (Hardware Auto Focus: off).
4. Under the “Saving” tab select or create the directory folder where the files should be saved. Assign a name to the file.
5. Under the “Wave Length” tab select the appropriate illumination and adjust exposure and gain. Use “YokoQuad Red” (or an equivalent illumination setting for mRFP imaging) with an exposure between 100 and 300 msec and a camera gain between 100 and 300, depending on the individual sample (assessed by using the live image).
6. Under the “Timelapse” tab select “Number of time points” = 301, “Duration” = 5 min and “Time/Interval” = 1 sec.
7. Under the “Journals” tab select Journal: “AFC SET Z HOLD” and “AFC Return to Z HOLD”, Type: “Special” (twice), Initial Point: “Start of time point” and “End of time point”. This autofocus option is important to image the same section over a longer period of time.
8. When the setup is done, press “Acquire”. The timelapse video is safed as separate TIFF files.
9. Open all .tiff files of a given time series in ImageJ. Go to “Image” →“Stacks”→“Images to Stacks”. Optionally, adjust brightness and contrast, add size bar, etc. Export the movie under “File”→“Save as”→“AVI…” (for an example, see Video 1 and 2 corresponding to **Figure 1**).

2. Using Folding Sensors and Stress Reporters to Investigate Cell Autonomous and Non cell Autonomous Affects on Proteostasis and Toxicity

1. Generate transgenic lines that coexpress a folding sensor or stress reporter together with the prion-like protein. For methods on how to establish crosses or generate transgenic lines, see[48,49,52]. See **Table 1** for a list of *C. elegans* strains that can be used.
2. Prepare synchronized populations of transgenic animals and grow them until the desired age as described above (section 1.2)[50].
3. Using a stereomicroscope, examine the respective phenotype of the folding sensor or stress reporter.
    1. For the folding sensor, determine the number of animals harboring aggregates on each day after synchronization (for an example, see **Figure 2E** and **F**).
    2. For the stress reporter, test if the coexpression of the prion-like protein results in an increased fluorescence of the reporter (for an example, see **Figure 3**).

3. Genome-wide Screen for Suppression of Prion-induced Toxicity in *C. elegans*

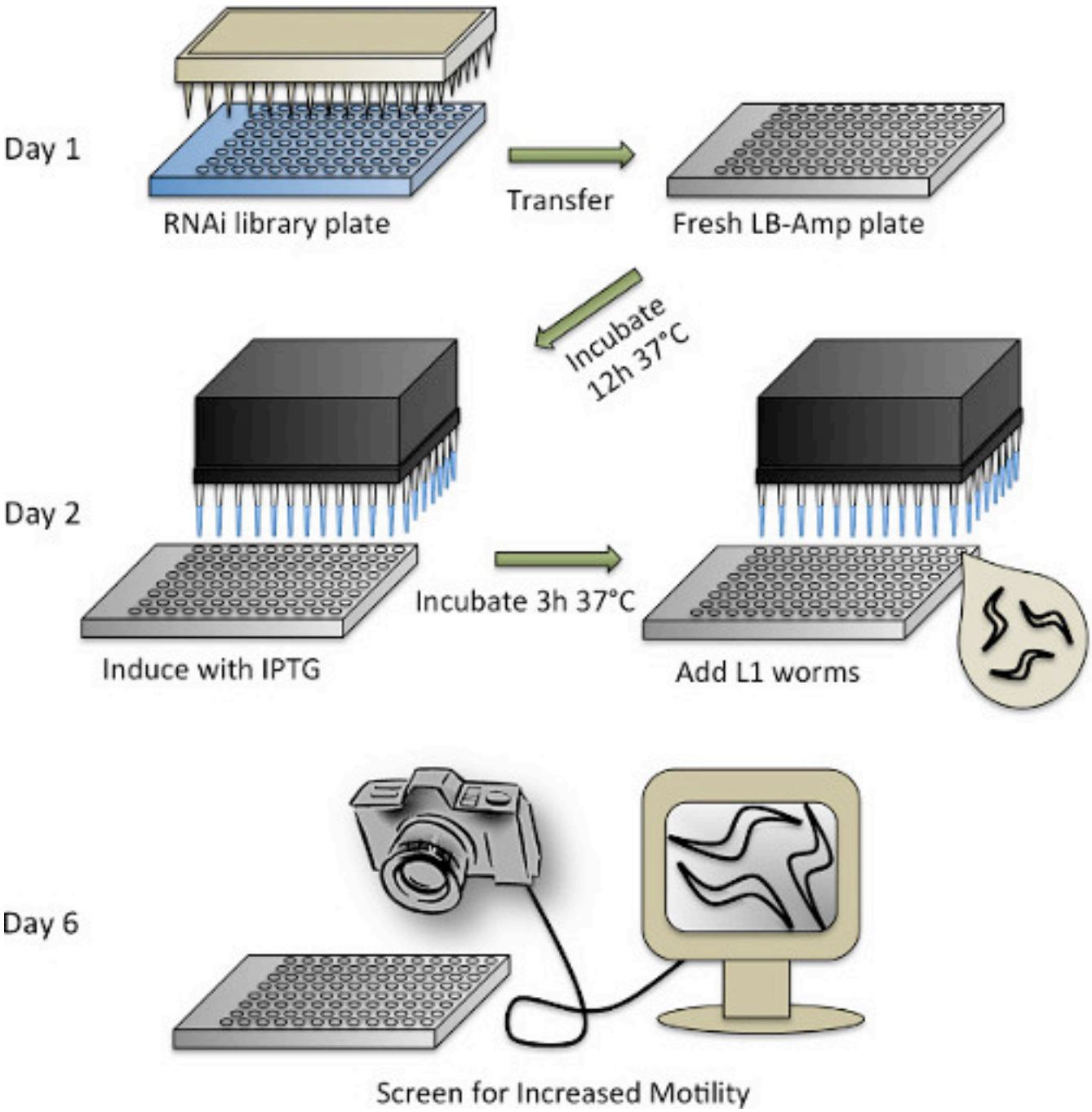

Figure 4. Schematic representation of the RNAi screening protocol. See protocol section 3 for a detailed description of the individual steps.

1. Synchronization of *C. elegans* worms and duplication of RNAi library
    1. For the RNAi screen, use the Ahringer RNAi library (or the Vidal RNAi library)[53,54]. Rearray the RNAi library from the original 384 well format into 96 well plates by filling the plates with 100 µl LB-amp media (50 µg/ml Ampicillin in LB) supplemented with 10% glycerol and inoculate using a 96-pin replicator. Grow at 37 °C O/N with agitation and store at -80 °C.
    2. Maintain *C. elegans* WT and transgenic lines at 20 °C on NGM plates seeded with OP50 *E. coli* bacteria according to standard methods[47].
    3. Synchronize prion domain transgenic and WT (control) nematodes by bleaching (see section 1.2).
    4. On the same day that the worms are bleached, prepare LB media supplemented with 50 µg/ml ampicillin. Use an automated reagent dispenser to dispense (or pipette manually) 65 µl of the LB-amp media into each well of a 96 well plate.
    5. Remove 96 well Ahringer RNAi library plates from -80 °C and bring them to a sterile hood lined with paper towels. Immediately remove the seal-tape by holding the plate upside down while plates are still frozen, being careful to avoid contamination from ice on the outside of the plates. Reinvert the plates and let them thaw for about 30 min.

6. Dip one sterile 96 pin replicator into one RNAi library plate, and then into one fresh LB-amp plate. Use a fresh sterile replicator for each plate. Seal all plates with adhesive foil tape and return the library plates to -80 °C. The replicators can be soaked in bleach, rinsed, and autoclaved to be used again.
7. Allow duplicated RNAi plates to grow O/N in an incubator set to 37 °C and 300 rpm. To use HT115 *E. coli* bacteria harboring the empty vector (L4440) as a control, grow it separately in a culture tube and then pipette 65 µl of the culture with a multichannel pipette into one quarter of two 96 well plates.

2. Induction of bacterial dsRNA production and addition of worms
    1. Dilute Isopropyl-β-D-thiogalactopyranosid (IPTG) to a 5 mM concentration in ddH_2O. Use an automated workstation with a multichannel head to dispense (or pipet manually) 10 µl of diluted IPTG into each well of the RNAi bacteria and the control plates. Reseal and place the plates back into the incubator. Let them shake for 3 hr at 37 °C.
    2. While bacteria are shaking, prepare the worms. Mix the M9/worm suspension well, and pipette a small sample (~5 - 10 µl) to a glass microscope slide. Count the number of worms under a stereomicroscope and calculate the number of worms per µl.
    3. Using sterile technique, prepare a solution of supplemented M9 (M9+) with the following final concentrations: 0.20 mg/ml IPTG, 8.0 µg/ml Cholesterol, 50 µg/ml Ampicillin, 9.6 µg/ml Tetracycline, 0.0835 µg/ml Fungizone, and 15 worms per 50 µl.
        1. Make separate solutions for prion domain transgenic and WT worms. The final volume of M9+ worm solution needed will depend on the number of RNAi plates copied (see below), plus ~30 ml of dead volume that will remain in the reservoir, if an automated dispenser is used.
    4. After the 3 hr induction of bacterial dsRNA production, take the plates out of the incubator and let them cool to RT (~30 min) to avoid heat stressing the animals.
    5. Dispense 50 µl M9+ prion domain transgenic worm solution to each well of the RNAi plates and one of the empty vector control plates. Make sure to mix the worm solution before each step as the animals tend to sediment to the bottom of the reservoir.
    6. Dispense WT worms into the second control plate. Leave the plates unsealed to allow aeration. To keep the liquid culture from evaporating, stack 4 - 5 plates together and wrap with a damp paper towel and aluminum foil. Incubate at 200 rpm at 20 °C for 4 days.

3. Scoring
    NOTE: After 4 days in the incubator, the worms will be at the second day of adulthood and are ready to screen. Let the animals adjust to non shaking conditions for 30 min before screening to ensure undisturbed thrashing.
    1. Using a Falcon 4M60 camera connected to a computer with a monitor, screen visually for increased thrashing as compared with control treated prion domain transgenic animals.
    2. Compile a list of preliminary hits to confirm using wrMTrck (see next section).

4. Confirmation of Preliminary Screen Hits

1. Motility assay on solid plates
    1. Prepare plates with NGM supplemented with 100 µg/ml ampicillin, 12.5 µg/ml tetracycline and 1 mM IPTG, according to standard methods[47]. If possible, use a plate-pouring machine to assure all plates have the same height of media, which will allow for a more streamlined video acquisition process.
    2. Grow the different RNAi clones in ~1 ml LB + 50 µg/ml ampicillin, O/N at 37 °C and 250 rpm.
    3. The next day, induce the expression of the dsRNA with 1 mM IPTG for 3 hr. Seed the plates with 150 µl of each RNAi bacterial clone, spread into a thin layer. Let the bacteria dry for 2 days at RT in the dark. Prepare 3 plates per RNAi clone.
    4. Synchronize the worm population by bleaching according to standard methods[50] (see section 1.2), and let the eggs hatch O/N in M9 media.
    5. Take a sample of the worm suspension and determine the amount of nematodes per µl at the stereomicroscope. Then, pipette the proper volume of M9 plus worms into each experimental plate so that it contains 25 - 30 L1 worms. Grow the nematodes at 20 °C for 4 days until the worms reach day 2 of adulthood.

2. Quantitative analysis of worm motility with the wrMTrck plugin for ImageJ
    NOTE: The videos were recorded using a stereomicroscope at 10X magnification with a Hamamatsu Orca-R2 digital camera C10600-10B and the Hamamatsu Simple PCI imaging software.
    1. Turn on the camera and the Simple PCI imaging software. Click on “Live” to allow for adjustment of the imaging conditions.
    2. Set up the video conditions as follows: Gain = 0; Light Mode = High; Speed Index = 1; Binning = 2. Click “Auto Expose” and then adjust the lighting conditions, moving the microscope mirrors and the brightness and contrast dials.
        NOTE: The video needs to have a high contrast without being overexposed, so that the animals appear as black shapes on a bright background.
    3. Click on “Time Scan” and choose a folder and a file name. Set “Field Delay” to 20 msec and “Stop at Time” to 30 sec. Press “Live Review” in order to choose the area of the plate to record (where most worms are). Tap the plate 3 or 4 times on the stage, quickly confirm its position in the field of view and press “Start”.
    4. After the movie finishes recording, right click on the image and choose “Export Montage Sequence” to export the movie from a .cxd format to an .avi.

3. Analyzing the motility videos
    1. Open the ImageJ software, go to the “Plugins” tab, then “wrmtrck” and select “wrMTrck Batch”. Select the directory containing all the files to be analyzed.
    2. In the main input window of wrMTrck_Batch, load the input values as detailed in **Figure 5C**. Explanation for each of the parameters can be found in the instructions that accompany the plugin. Click “OK” and let the movement analysis run.

3. To curate the results and confirm that all detected tracks are from actual *C. elegans* and eliminate artifacts, open each of the .txt files created for each movie and copy the information to a data analysis software file. Open the "*_labels.zip" files created and run the resulting "*_labels.tif" to manually check and eliminate false worm tracks.

Representative Results

Monitoring intercellular spreading of prion-like proteins by *in vivo* time-lapse imaging

Transgenic *C. elegans* lines expressing the prion domain are particularly well suited for the analysis of certain aspects of prion-like proteins, *e.g.*, cell-to-cell transmission and non cell autonomous toxicity. The transparency of the animals enables tracking of fluorescently tagged proteins from within the living organism at every stage of life. Taking advantage of this, movement of prion-like proteins across cells and tissues using a fluorescence microscope are visualized. A 63X or 100X/1.4NA oil objective is necessary to resolve the vesicular structures. Importantly, the prion domain has to be tagged with mRFP, in order to remain fluorescently visible within these presumably acidic vesicles[40]. Yellow fluorescent protein (YFP), which is often used as a tag, is not suitable because it is quenched in a low pH environment[40,55]. Strain AM815 expresses RFP-tagged R2E2 (a highly aggregation-prone and toxic form of the prion domain NM) that accumulates in tubular vesicles, while the RFP tag alone remains soluble (**Figure 1A** and **B**). Using *in vivo* time-lapse imaging, it could be observed that these tubular vesicles are transported within and between cells[40] (**Figure 1C** and **D**, **Video 1** and **2**) [place links to Video 1 and 2 here].

Using folding sensors and stress reporters to investigate cell autonomous and non-cell autonomous effects on proteostasis and toxicity

Prions are able to cross seed related proteins and disrupt the cellular protein folding environment. This can be revealed through the coexpression of appropriate folding sensors. Folding sensors are non-essential metastable proteins that depend on a functional proteostasis network to fold correctly. Some examples are the well-known firefly luciferase and proteins harboring temperature-sensitive (ts) mutations[56-66]. A disruption of proteostasis leads to misfolding of the reporter, which can be detected by visual examination of aggregates or by exposure of the respective ts mutant phenotype at permissive temperatures. Stretches of polyglutamine (polyQ) with a length at the threshold of aggregation (around 40 residues) are also often used because they exhibit an age-dependent aggregation[67-69]. Earlier onset of aggregation reveals a compromised folding environment. Here, we employed a prion mutant RΔ2-5 that remains soluble when expressed in *C. elegans* body wall muscle (BWM) cells and intestine[40] (**Figure 2A** and **C**). Upon simultaneous expression with R2E2 in BWM cells, RΔ2-5 readily aggregates (**Figure 2B**), revealing a cell autonomous effect of R2E2 on the protein folding environment. The widespread effect on proteostasis and induction of misfolding across tissues can be evaluated by expression of the folding sensor in a distinct tissue that does not express the highly aggregation-prone form of the prion domain. R2E2 was expressed under a BWM cell specific promoter (*myo-3p*), whereas RΔ2-5 was expressed under an intestine-specific promoter (*vha-6p*). Aggregation of intestinal RΔ2-5 demonstrates that R2E2 affects protein folding in a non cell autonomous manner[40] (**Figure 2D**). Instead of using RΔ2-5, where aggregates can only be detected at high resolution, the use of polyQ44 expressed in the intestine (Q44i) allows visualization of aggregates at low resolution under a stereomicroscope (**Figure 2E** and **F**). Furthermore, this enables a quantification of animals with aggregates, as well as a quantification of the number of aggregates.

To investigate non cell autonomous toxicity of the prion domain, we previously examined neighboring tissues that do not express R2E2 by electron microscopy and found that expression of the prion domain in muscle cells leads to a non cell autonomous disruption of mitochondrial integrity in adjacent tissues, such as the intestine[40]. Mitochondrial dysfunction results in increased reactive oxygen species (ROS) production and oxidative stress. A noninvasive way to visualize induction of the oxidative stress response is to use an oxidative stress inducible reporter[70]. The strain CF1553 expresses green fluorescent protein (GFP) under the oxidative stress inducible promoter *sod-3*[70]. When crossed to animals expressing the prion domain R2E2 in BWM cells, the reporter was significantly upregulated in BWM cells as well as in numerous non-BWM tissues (**Figure 3**). This strain can be used to examine if certain candidate genes influence this non cell autonomous induction of the oxidative stress response. **Table 1** provides a list of *C. elegans* strains expressing folding sensors and stress reporters that can be used analogously.

Genome-wide screen for suppression of prion-induced toxicity in *C. elegans*

The complex toxicity phenotype of the prion domain expressed in *C. elegans* is particularly interesting because of the lack of discernible toxicity observed in most *in vitro* prion models[71]. This model might reveal new pathways that can influence the toxicity associated with prions in metazoans. To address this, we have screened for genes that, when RNAi-depleted, would improve the motility defect of R2E2 transgenic animals. Control treated WT worms can be used as a positive control, although most candidate genes will not provide a full movement phenotype rescue, due to the variable RNAi penetrance and the high toxicity of the transgene. The animals were treated for 4 days with RNAi, from the first larval state L1 to day 2 of adulthood. By that time, the thrashing of untreated R2E2 animals is significantly slower than the thrashing of WT animals, which is important because we are screening for an improvement of motility. F1 progeny will be present (~L1s), but is easy to distinguish from the P0 generation. Only the P0 generation is scored. This initial screen is visual and non quantitative and therefore, a low threshold was used to identify preliminary hits, meaning that every bacterial RNAi clone that seemed to increase the thrashing of prion-expressing animals was retested in a quantitative crawling assay. **Figure 4** outlines the main steps of the screen setup. The high resolution of the Falcon 4M60 camera enabled a visual screening of a quarter of the plate at a time on a computer screen, which allowed the screen to be completed more efficiently. While helpful, this is not necessary. The visual examination of worm thrashing can also be performed by using a stereoscope at low magnification (10X).

Confirmation of preliminary screen hits

High throughput screens are performed as an approach that allows analyzing genome wide effects to obtain a primary list of candidate genes that can be refined by complementary methods. Validation of the screen results is therefore essential to eliminate possible false positives, which might result from performing a screen with only one experimental sample per RNAi. R2E2 transgenic animals were fed with the RNAi clones of primary hits and measured their speed on NGM plates on the second day of adulthood, as a quantifiable readout of motility and decreased toxicity. We used the wrMTrck plugin for ImageJ, developed in our laboratory, which accurately identifies *C. elegans* in videos and follows their

movement. The wrMTrck plugin and scripts for automated analysis are open-source and publicly available at http://www.phage.dk/plugins/wrmtrck.html, along with detailed instructions on how to use it. After downloading, copy the whole wrMTrck folder to the Plugins folder of ImageJ. This protocol describes the wrMTrck_Batch method, preferred for analyzing a large number of videos at a time, but instructions for a manual, movie by movie, analysis are also available with the plugin download. WrMTrck_Batch converts an original video (**Figure 5A**) into a binary format with background subtraction and each worm is assigned a track. Each of the processed videos can later be viewed with these tracks superimposed, in order to manually eliminate any artifacts that were falsely identified as worms (*e. g.*, track 1 in **Figure 5B**). One effective way to eliminate background artifacts (indicated with an arrow on **Figure 5B**) is to carefully choose the minimum and maximum size of the objects to be identified (**Figure 5C**). From the different outputs of the wrMTrck plugin, we use the body lengths per second (BLPS) parameter which measures the average speed of each animal, represented by the length of each track divided by the body length of each object, thus normalizing for potential differences in size of the nematodes (**Figure 5D**). Using this method, we identified 35 suppressors of prion-induced toxicity (sopt) that increased the motility phenotype in R2E2 expressing *C. elegans* to at least 133% and up to 256% when compared to empty vector-treated worms (**Figure 6**). These sopt genes represent the final confirmed hits that resulted from our high throughput screening efforts.

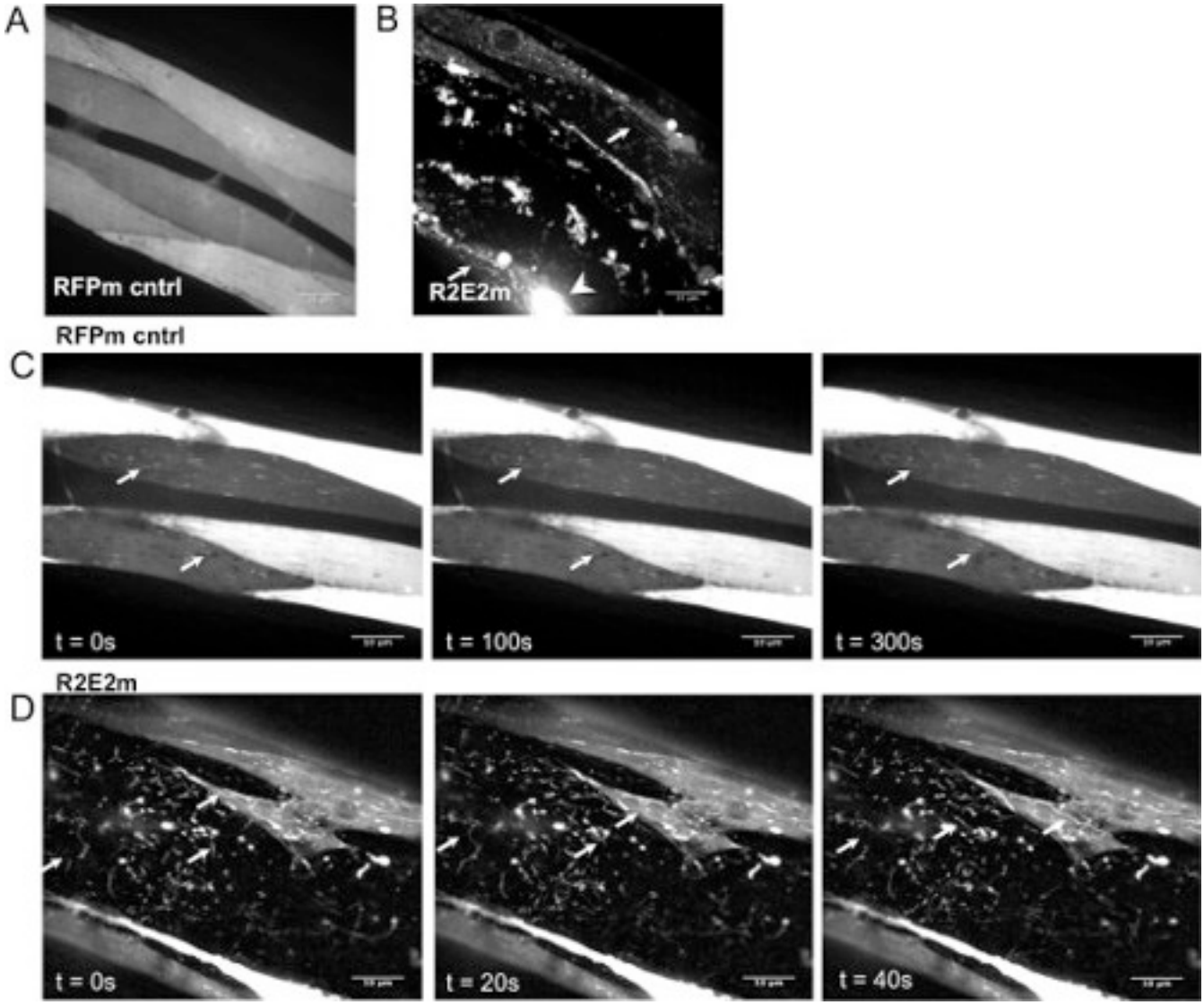

Figure 1. The prion domain spreads between cells and tissues in *C. elegans* by vesicular transport. **(A)** Collapsed confocal z-stacks of nematodes expressing RFP in body wall muscle (BWM) cells (RFPm). **(B)** Collapsed confocal z-stacks of nematodes expressing the highly toxic and aggregation prone NM variant, R2E2, in BWM cells (R2E2m). Arrows indicate tubular vesicles, arrowhead indicates aggregate. **(C +D)** Time-lapse series of animals expressing RFPm **(C)** and R2E2m **(D)**. Arrows indicate areas of vesicular movement. RFPm exhibits mostly a diffuse staining. Even when RFPm is found in vesicles, these barely move. R2E2m localizes to numerous vesicles that are transported within and between cells. Scale bars: 10 µm. The accompanying Videos 1 and 2 [place links to Video 1 and 2 here] correspond to the Figures 1C and D, respectively.

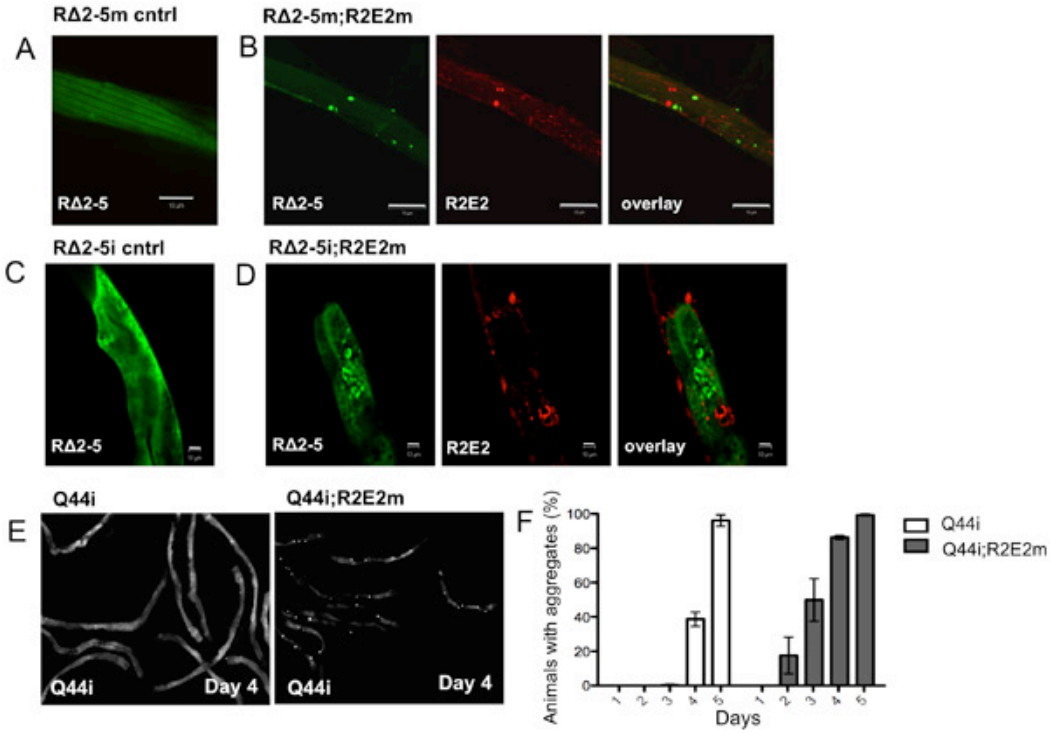

Figure 2. Folding sensors reveal the widespread effect of the prion domain on proteostasis. (A+B) Coexpression of R2E2m promotes RΔ2-5m aggregation. Confocal images of **(A)** RΔ2-5m control and **(B)** RΔ2-5m coexpressed with R2E2m in BWM cells. **(C+D)** Muscle expressed R2E2m promotes intestinal RΔ2-5i aggregation. **(C)** Confocal image of control animal expressing RΔ2-5i in intestinal cells. **(D)** Confocal image of animals expressing R2E2m in BWM cells and RΔ2-5i in the intestine. Scale bars: 10 µm. **(E+F)** R2E2m induces non cell autonomous aggregation of Q44i. **(E)** Representative fluorescent images of Q44i and Q44i;R2E2m animals 4 days after transferring synchronized L1 larvae onto fresh OP50-seeded NGM plates. The expression of R2E2 in BWM cells leads to an earlier onset of Q44i aggregation in the intestine. **(F)** Quantification of animals with aggregates (in %) on indicated days after synchronization. Error bars represent S.D. This figure has been modified from[40].

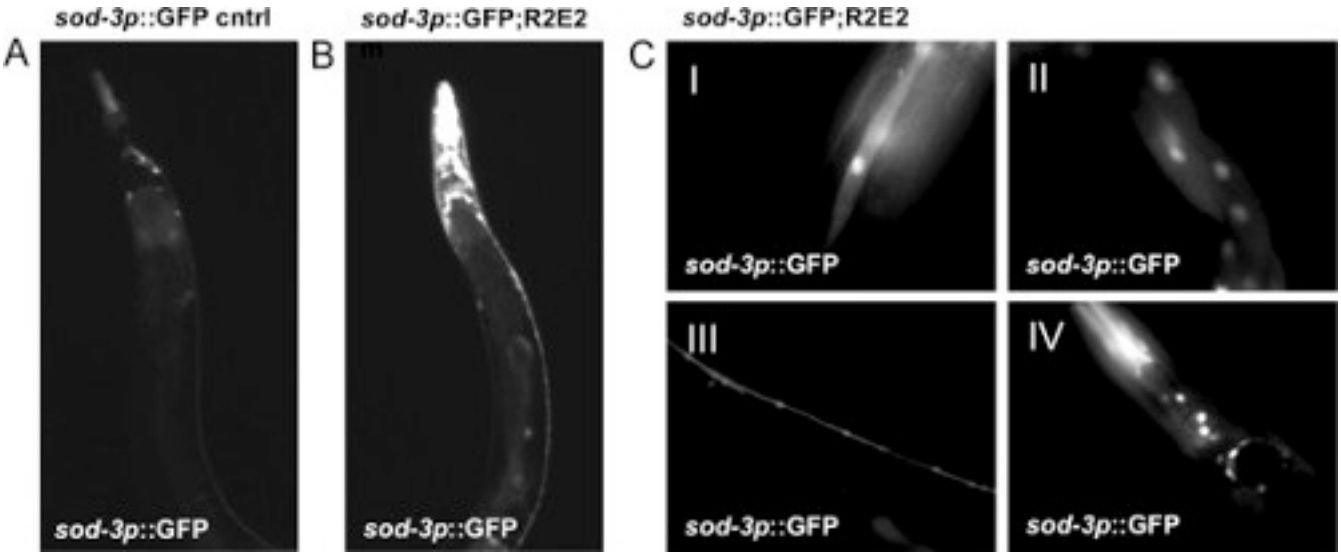

Figure 3. The sod-3p::GFP transcriptional stress reporter reveals that the prion domain causes cell autonomous and non cell autonomous induction of oxidative stress. (A+B) Representative fluorescent images (using the same exposure time) of *sod-3p*::GFP expressing control animals **(A)** and *sod-3p*::GFP;R2E2m animals **(B)** on day 2 of adulthood. **(C)** The expression of R2E2 in BWM cells leads to an induction of the reporter not only in BWM cells (I), but also in the intestine (II), nerve cord (III), pharynx and head neurons (IV).

A

B

C

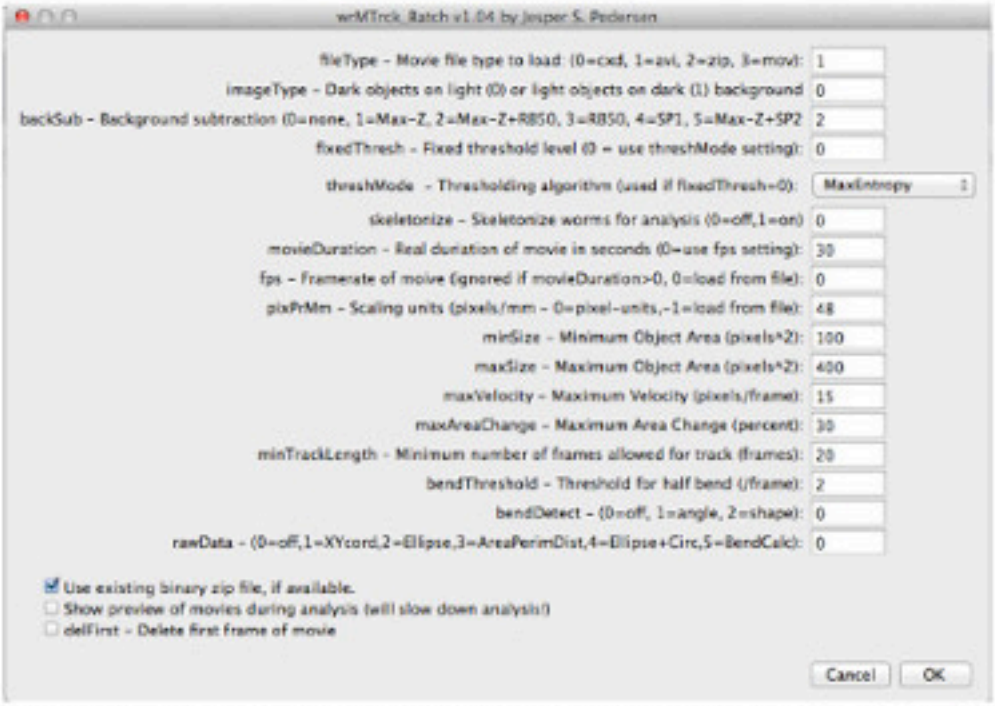

D

Track	Length	Distance	#Frames	1stFrame	time(s)	MaxSpeed	AvgArea	StdArea	AvgPerim	StdPerim	AvgSpeed	BLPS	avgX	avgX
1	0.32612	6.91E-04	150	0	29.4118	0.029917	0.05547	0.00068	1.71219	0.08056	0.011088	0.01295	12.8812	0.75329
2	0.49102	0.44503	40	0	7.84314	0.165354	0.04847	0.00201	1.62926	0.04317	0.062605	0.07685	9.74414	0.61602
3	3.27038	1.49141	150	0	29.4118	0.348603	0.05946	0.00219	1.76429	0.03037	0.111193	0.12605	12.0155	4.68385
4	2.92103	0.75899	150	0	29.4118	0.43749	0.05289	0.00352	1.66398	0.09612	0.099315	0.10656	9.80023	8.01814
5	1.58955	1.30195	150	0	29.4118	0.192552	0.05933	0.00246	1.76325	0.03648	0.054045	0.0613	11.3217	7.28241
6	2.19531	0.87069	150	0	29.4118	0.187092	0.05138	0.00169	1.59822	0.03024	0.07464	0.0934	8.73344	9.74189
7	0.86761	0.73583	144	6	28.2353	0.132468	0.05363	0.00273	1.67081	0.06401	0.030728	0.03678	13.2277	5.04649
8	0.81857	0.70087	141	9	27.6471	0.170191	0.05262	0.00152	1.73313	0.0288	0.029608	0.03417	2.54034	9.76137
9	0.37452	0.37256	23	12	4.5098	0.146462	0.04608	0.00107	1.535	0.02783	0.083045	0.1062	11.2585	1.07702
10	0.37423	0.1808	35	36	6.86275	0.127115	0.04524	0.00101	1.51815	0.03063	0.054531	0.07184	10.9763	1.06248
11	0.85893	0.04137	99	51	19.4118	0.196147	0.0488	0.0023	1.6191	0.04386	0.044248	0.05466	9.82386	0.47192
12	2.23996	1.65106	92	58	18.0392	0.236091	0.05745	0.0026	1.69199	0.02605	0.124172	0.14678	3.81271	9.76722
13	0.46285	0.03964	48	91	9.41177	0.206581	0.04516	0.00119	1.50522	0.02994	0.049177	0.06534	10.6998	1.01519

Figure 5. Analysis of worm movement with the wrMTrck plugin for ImageJ. (A) Example of an input movie generated by using an appropriate magnification (~10X) to monitor several animals at a time. **(B)** "*_labels.tif" files are an output of wrMTrck_Batch and allow for manual curation of analysis results. Arrow indicates an object that was correctly excluded from the analysis due to an appropriate choice of minimum and maximum size parameters. **(C)** Input window of wrMTrck_Batch, showing parameters used for this protocol. These parameters need to be adjusted according to the individual microscope and movie settings. **(D)** Output results from movement analysis of **(B)**, with the BLPS column highlighted in yellow. Please click here to view a larger version of this figure.

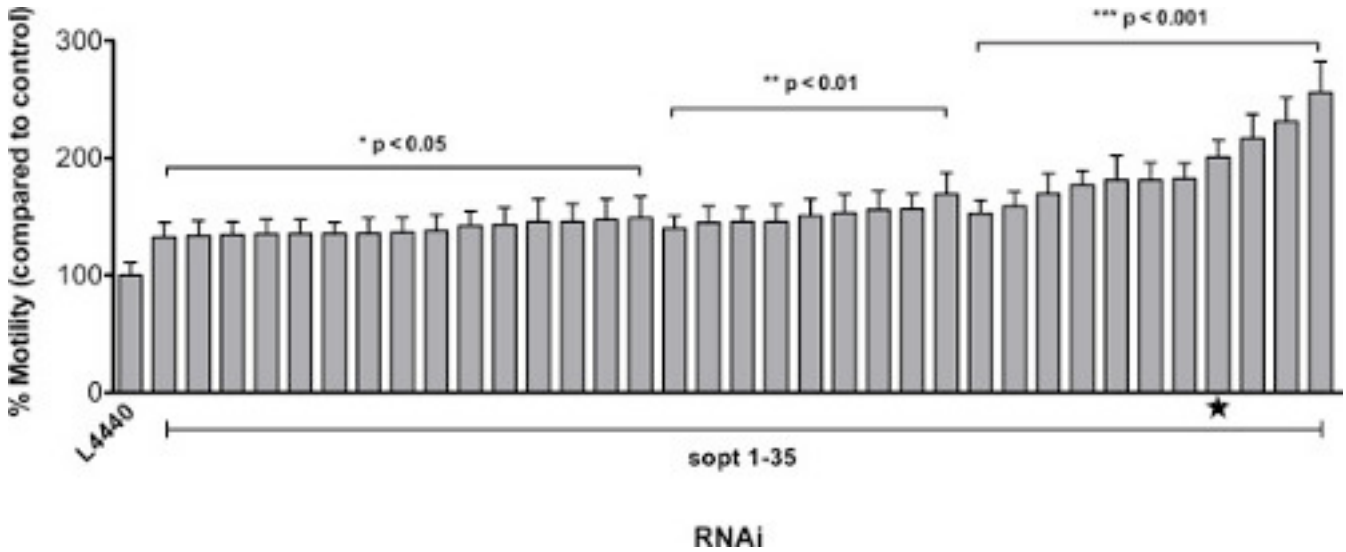

Figure 6. R2E2 worms treated with RNAi clones that are supressors of prion-induced toxicity (sopt) show improved motility. Motility is shown as relative BLPS when compared to the negative control (empty vector). Shown are all statistically significant (student t-test) RNAi clones identified in the HTP screen. ★ represents the hit shown as an example in **Figure 5**. Results are from 3 movies, with 17 <n <53 tracks per condition. Error bars represent SEM.

Table 1. *C. elegans* strains expressing folding sensors and stress reporters.

Strain name	genotype	Comments	Strain source
Folding sensors			
transgenes			
AM140	*unc-54p::polyQ35::yfp*	muscle-specific expression of polyQ35, age dependent aggregation	CGC or Morimoto lab
AM141	*unc-54p::polyQ40::yfp*	muscle-specific expression of polyQ40, age dependent aggregation	CGC or Morimoto lab
AM801	*unc-54p::RΔ2-5::yfp*	muscle-specific expression of nucleation incompetent prion domain	Morimoto lab
OG412	*vha-6p::polyQ44::yfp*	intestine-specific expression of polyQ44, age dependent aggregation	CGC
AM809	*vha-6p::RΔ2-5::gfp; myo-2p::mcherry*	intestine-specific expression of nucleation incompetent prion domain	Morimoto lab
AM47	*F25B3.3p::polyQ40::cfp*	neuron-specific expression of polyQ40, cell type specific aggregation	Morimoto lab
AM982	*unc54p::luciferase::yfp*	muscle-specific expression of WT firefly luciferase	Morimoto lab
	myo-3p::luciferase::gfp; rol-6	muscle-specific expression of WT firefly luciferase	Behl lab
	sng-1p::luciferase::gfp; rol-6	muscle-specific expression of WT firefly luciferase	Behl lab
FUH55	*unc54p::FLUC::egfp; rol-6*	muscle-specific expression of WT firefly luciferase	Hartl lab
FUH134	*unc54p::FLUCSM::egfp; rol-6*	muscle-specific expression of R188Q mutant firefly luciferase	Hartl lab

FUH135	*unc54p::FLUCDM::egfp; rol-6*	muscle-specific expression of R188Q+R261Q double mutant firefly luciferase	Hartl lab
FUH48	*F25B3.3p::FLUC::egfp; rol-6*	neuron-specific expression of WT firefly luciferase	Hartl lab
FUH136	*F25B3.3p::FLUCSM::egfp; rol-6*	neuron-specific expression of R188Q mutant firefly luciferase	Hartl lab
FUH137	*F25B3.3p::FLUCDM::egfp; rol-6*	neuron-specific expression of R188Q+R261Q double mutant firefly luciferase	Hartl lab
ts mutants			
CB1402	*unc-15(e1402) I*	Paramyosin(ts), temperature sensitive Unc-paralyzed, Let	CGC
CB1157	*unc-54(e1157) I*	Myosin(ts), temperature sensitive Unc	CGC
CB1301	*unc-54(e1301) I*	Myosin(ts), temperature sensitive Unc	CGC
CB286	*unc-45(e286) III*	Unc-45(ts), temperature sensitive, slow moving Unc, Egl	CGC
HE250	*unc-52(e669su250) II*	Perlecan(ts), temperature sensitive Unc, stiff paralysis	CGC
SD551	*let-60(ga89) IV*	Ras(ts), temperature sensitive Muv, Ste, Let, Lva, Osm	CGC
CX51	*dyn-1(ky51) X*	Dynamin(ts), temperature sensitive Unc	CGC
CW152	*gas-1(fc21) X*	Gas-1(ts), temperature sensitive EtOH sensitivity	CGC
ZZ26	*unc-63(x26) I*	Acetylcholine receptor(ts), temperature sensitive levamisole resistance	CGC
stress reporters			
CL2070	*hsp-16.2p::gfp;rol-6*	thermal stress; UPR^{cyto}	CGC
TJ375	*hsp-16.2p::gfp*	thermal stress; UPR^{cyto}	CGC
TJ3000, TJ3001	*hsp-16.2p::gfp; Cbr-unc-119(+)*	thermal stress; UPR^{cyto}	CGC
AM446	*hsp70p::gfp;rol-6*	thermal stress; UPR^{cyto}	Morimoto lab
AM722	*hsp70p::mcherry; myo-2p::cfp*	thermal stress; UPR^{cyto}	Morimoto lab
AM799	*hsp90p::gfp*	thermal stress; UPR^{cyto}	Morimoto lab
OG497	*hsf-1p::hsf-1::gfp; Cbr-unc-119(+)*	thermal stress; UPR^{cyto}	CGC
CF1553	*sod-3p::gfp;rol-6*	oxidative stress	CGC
KN259	*sod-3p::gfp;rol-6*	oxidative stress	CGC
CL2166	*gst-4p::gfp::nls*	oxidative stress	CGC
LD1171	*gcs-1p::gfp;rol-6*	oxidative stress	CGC
LD1	*skn-1p::skn-1::gfp;rol-6*	oxidative stress	CGC
IG274	*nlp-29p::gfp*	osmotic stress	CGC
BC20309	*mtl-1p::gfp*	metal stress	Baillie lab
BC20342	*mtl-2p::gfp*	metal stress	Baillie lab
BC20314	*elt-2p::gfp*	metal stress	Baillie lab
SJ4005	*hsp-4p::gfp*	UPR^{ER}	CGC
SJ4100	*hsp-6p::gfp*	UPR^{mito}	CGC

SJ4058	*hsp-60p::gfp*	UPR^{mito}	CGC

CGC: Caenorhabditis Genetics Center; ts = temperature sensitive; UPR = unfolded protein response; cyto = cytosolic; mito = mitochondrial; ER = endoplasmic reticulum.

Discussion

The methods described here help to illustrate spreading and the complex cell autonomous and non cell autonomous toxicity of prion-like proteins. We recently discovered that an aggregation-prone cytosolic prion domain is taken up into membrane-bound vesicles in an autophagy related process. A specific subset of these vesicles transports the prion domain within and between cells and tissues[40]. The key to monitor their movement in the living animal is that the protein has to be tagged with mRFP, because only mRFP-tagged proteins were visible in these presumably acidic vesicles. Using the same approach, we are currently investigating the potential prion-like behavior of certain disease-related proteins, such as superoxide dismutase 1 (SOD1) (linked to ALS), alpha-synuclein (linked to PD) or TAR DNA-binding protein 43 (TDP-43) (linked to ALS). Although this intercellular transport within vesicles seems to be used by several other proteins, there might be additional pathways that allow spreading.

The use of well characterized folding sensors is a powerful tool to monitor effects on the cellular protein folding environment in *C. elegans*[63-66]. Here we have shown how to use the age dependent accumulation of fluorescently tagged aggregation prone proteins expressed under tissue-specific promoters to visually monitor the folding capacity of distinct tissues simultaneously. Other possibilities to study the organismal proteostasis network include the use of endogenous ts mutant proteins. These metastable proteins will function normally at the permissive temperature (15 °C), but misfold and become nonfunctional at the restrictive temperature (25 °C), exhibiting their characteristic mutant phenotype. In the presence of an aggregation prone protein or during aging, the ts mutant phenotype gets exposed even at permissive conditions[63-66]. Some of these ts mutants are expressed in only a subset of tissues or exhibit tissue-specific phenotypes, making these particularly useful to test for cell autonomous and non cell autonomous proteotoxic effects. For example, a ts mutant of LET-60, a member of the GTP-binding RAS protooncogene family, Ras(ts), is ubiquitously expressed, but shows tissue-specific mutant phenotypes[63,66]. By using this ts mutant, the effect of polyQ expansions on the cellular proteostasis was shown to be cell autonomous[63]. Expression of polyQ in the genetic background of *ras(ts)* revealed only the mutant phenotype specific to the tissue in which the protein was expressed. The exposure of multiple mutant phenotypes would indicate that a protein has non-cell autonomous proteotoxic effects.

Additionally, to test for effects on cellular stress pathways, there is a large selection of *in vivo* fluorescent stress reporters in *C. elegans*[72]. These are usually transcriptional reporters that express green fluorescent protein (GFP) under a stress-inducible promoter, such as *hsp-16.2p* or *sod-3p*, which report on thermal or oxidative stress, respectively[72]. By using appropriate reporters in combination with prion-like proteins, one can monitor a potential induction of stress responses in tissues other than the one expressing the respective transgene. One caveat, however, is that these stress reporters are often not sensitive enough to reveal subtle upregulation of a given pathway (unpublished observations).

On our quest to examine whether genes that influence the non-cell autonomous toxicity also affect protein spreading, we started by screening for genes that, when knocked down, would ameliorate movement defects. Using visual evaluation of swimming rates as a read-out, we were able to comfortably assay ~25 plates per session and perform two rounds of this protocol per week, resulting in the completion of the initial screen within 6 weeks. The confirmation of the hits, by quantitative analysis of worm movement on solid plates, in triplicates, using wrMTrck was performed in an additional 3 weeks. One caveat, however, is that by using crawling in plates instead of swimming in liquid media as a read-out one might lose certain candidate genes, as swimming and crawling are not identical motions and can be influenced by distinct pathways[73]. Thus, if some candidate genes cannot be confirmed on solid plates, they should be re-tested in liquid media, where swimming can be quantified by counting the thrashing frequency within a given time.

The screening protocol described here uses automated liquid handling workstations, which greatly reduces variability. The disadvantage is that an excess of fluids for the reservoir of the robots is needed, which might not always be feasible. This screening setup can be easily adapted for other screens in *C. elegans* that use thrashing as a read-out.This screen was not designed to directly identify genes that influence the spreading or non cell autonomous toxicity of the prion domain, as genome wide screens should be simple in design, so as to be performed in a timely manner. Motility defects can originate not only from muscular, but also from neuronal damage and from a number of other gene defects[53]. Thus, by using this readout, we might find not only modifiers of muscle-specific toxicity. We are currently testing the candidate genes for their effects on prion domain spreading and non cell autonomous toxicity using the methods described above. These experiments will eventually reveal whether transcellular spreading of protein aggregates is directly linked to the toxicity observed in other tissues or if cell-to-cell transmission and non cell autonomous toxicity can be uncoupled.

Taken together, the described methods can be used to examine the potential prion-like behavior of proteins at the cellular and organismal level using *C. elegans*.

Disclosures

The authors declare no competing financial interests.

Acknowledgements

We thank Cindy Voisine and Yoko Shibata for helpful discussion and critical comments on the manuscript. We acknowledge the High Throughput Analysis Laboratory (HTAL) and the Biological Imaging Facility (BIF) at Northwestern University for their assistance. This work was funded by grants from the National Institutes of Health (NIGMS, NIA, NINDS), the Ellison Medical Foundation, and the Daniel F. and Ada L. Rice Foundation (to R.I.M.). C.I.N.-K. was supported by the Deutsche Forschungsgemeinschaft (KR 3726/1-1).

References

1. Prusiner, S. B. Novel proteinaceous infectious particles cause scrapie. *Science.* **216** (4542), 136-144, doi:10.1126/science.6801762, (1982).
2. Jarrett, J. T., & Lansbury, P. T., Jr. Seeding 'one-dimensional crystallization' of amyloid: a pathogenic mechanism in Alzheimer's disease and scrapie. *Cell.* **73** (6), 1055-1058, doi:0092-8674(93)90635-4, (1993).
3. Caughey, B., Kocisko, D. A., Raymond, G. J., & Lansbury, P. T., Jr. Aggregates of scrapie-associated prion protein induce the cell-free conversion of protease-sensitive prion protein to the protease-resistant state. *Chem Biol.* **2** (12), 807-817, doi:10.1016/1074-5521(95)90087-X, (1995).
4. Wickner, R. B. [URE3] as an altered URE2 protein: evidence for a prion analog in Saccharomyces cerevisiae. *Science.* **264** (5158), 566-569, doi:10.1126/science.7909170, (1994).
5. Chien, P., Weissman, J. S., & DePace, A. H. Emerging principles of conformation-based prion inheritance. *Annu Rev Biochem.* **73**, 617-656, doi:10.1146/annurev.biochem.72.121801.161837, (2004).
6. Kimberlin, R. H., & Walker, C. A. Pathogenesis of mouse scrapie: patterns of agent replication in different parts of the CNS following intraperitoneal infection. *J R Soc Med.* **75** (8), 618-624, (1982).
7. Beekes, M., McBride, P. A., & Baldauf, E. Cerebral targeting indicates vagal spread of infection in hamsters fed with scrapie. *J Gen Virol.* **79** (3), 601-607, (1998).
8. Jucker, M., & Walker, L. C. Self-propagation of pathogenic protein aggregates in neurodegenerative diseases. *Nature.* **501** (7465), 45-51, doi:10.1038/nature12481, (2013).
9. Aguzzi, A. Cell biology: Beyond the prion principle. *Nature.* **459** (7249), 924-925, doi:10.1038/459924a, (2009).
10. Scherzinger, E. *et al.* Self-assembly of polyglutamine-containing huntingtin fragments into amyloid-like fibrils: implications for Huntington's disease pathology. *Proc Natl Acad Sci U S A.* **96** (8), 4604-4609, doi:10.1073/pnas.96.8.4604, (1999).
11. Wood, S. J. *et al.* alpha-synuclein fibrillogenesis is nucleation-dependent. Implications for the pathogenesis of Parkinson's disease. *J Biol Chem.* **274** (28), 19509-19512, (1999).
12. Wang, Y. Q. *et al.* Relationship between prion propensity and the rates of individual molecular steps of fibril assembly. *J Biol Chem.* **286** (14), 12101-12107, doi:10.1074/jbc.M110.208934, (2011).
13. Cushman, M., Johnson, B. S., King, O. D., Gitler, A. D., & Shorter, J. Prion-like disorders: blurring the divide between transmissibility and infectivity. *J Cell Sci.* **123** (8), 1191-1201, doi:10.1242/jcs.051672, (2010).
14. Tanaka, M., Collins, S. R., Toyama, B. H., & Weissman, J. S. The physical basis of how prion conformations determine strain phenotypes. *Nature.* **442** (7102), 585-589, doi:10.1038/nature04922, (2006).
15. Winkler, J., Tyedmers, J., Bukau, B., & Mogk, A. Chaperone networks in protein disaggregation and prion propagation. *J Struct Biol.* **179** (2), 152-160, doi:10.1016/j.jsb.2012.05.002, (2012).
16. Ilieva, H., Polymenidou, M., & Cleveland, D. W. Non-cell autonomous toxicity in neurodegenerative disorders: ALS and beyond. *J Cell Biol.* **187** (6), 761-772, doi:10.1083/jcb.200908164, (2009).
17. Nussbaum-Krammer, C. I., & Morimoto, R. I. Caenorhabditis elegans as a model system for studying non-cell-autonomous mechanisms in protein-misfolding diseases. *Dis Model Mech.* **7** (1), 31-39, doi:10.1242/dmm.013011, (2014).
18. Lino, M. M., Schneider, C., & Caroni, P. Accumulation of SOD1 mutants in postnatal motoneurons does not cause motoneuron pathology or motoneuron disease. *J Neurosci.* **22** (12), 4825-4832, (2002).
19. Li, J. Y. *et al.* Lewy bodies in grafted neurons in subjects with Parkinson's disease suggest host-to-graft disease propagation. *Nat Med.* **14** (5), 501-503, doi:10.1038/nm1746, (2008).
20. Desplats, P. *et al.* Inclusion formation and neuronal cell death through neuron-to-neuron transmission of alpha-synuclein. *Proc Natl Acad Sci U S A.* **106** (31), 13010-13015, doi:10.1073/pnas.0903691106, (2009).
21. Clement, A. M. *et al.* Wild-type nonneuronal cells extend survival of SOD1 mutant motor neurons in ALS mice. *Science.* **302** (5642), 113-117, doi:10.1126/science.1086071, (2003).
22. Gu, X. *et al.* Pathological cell-cell interactions elicited by a neuropathogenic form of mutant Huntingtin contribute to cortical pathogenesis in HD mice. *Neuron.* **46** (3), 433-444, doi:10.1016/j.neuron.2005.03.025, (2005).
23. Yamanaka, K. *et al.* Mutant SOD1 in cell types other than motor neurons and oligodendrocytes accelerates onset of disease in ALS mice. *Proc Natl Acad Sci U S A.* **105** (21), 7594-7599, doi:10.1073/pnas.0802556105, (2008).
24. Garden, G. A. *et al.* Polyglutamine-expanded ataxin-7 promotes non-cell-autonomous purkinje cell degeneration and displays proteolytic cleavage in ataxic transgenic mice. *J Neurosci.* **22** (12), 4897-4905, (2002).
25. Raeber, A. J. *et al.* Astrocyte-specific expression of hamster prion protein (PrP) renders PrP knockout mice susceptible to hamster scrapie. *EMBO J.* **16** (20), 6057-6065, doi:10.1093/emboj/16.20.6057, (1997).
26. Yazawa, I. *et al.* Mouse model of multiple system atrophy alpha-synuclein expression in oligodendrocytes causes glial and neuronal degeneration. *Neuron.* **45** (6), 847-859, doi:10.1016/j.neuron.2005.01.032, (2005).
27. Lobsiger, C. S., & Cleveland, D. W. Glial cells as intrinsic components of non-cell-autonomous neurodegenerative disease. *Nat Neurosci.* **10** (11), 1355-1360, doi:10.1038/nn1988, (2007).
28. Sambataro, F., & Pennuto, M. Cell-autonomous and non-cell-autonomous toxicity in polyglutamine diseases. *Prog Neurobiol.* **97** (2), 152-172, doi:10.1016/j.pneurobio.2011.10.003, (2012).
29. Polymenidou, M., & Cleveland, D. W. Prion-like spread of protein aggregates in neurodegeneration. *J Exp Med.* **209** (5), 889-893, doi:10.1084/jem.20120741, (2012).
30. Brundin, P., Melki, R., & Kopito, R. Prion-like transmission of protein aggregates in neurodegenerative diseases. *Nat Rev Mol Cell Biol.* **11** (4), 301-307, doi:10.1038/nrm2873, (2010).
31. Braak, H., Braak, E., & Bohl, J. Staging of Alzheimer-related cortical destruction. *Eur Neurol.* **33** (6), 403-408, (1993).
32. Meyer-Luehmann, M. *et al.* Exogenous induction of cerebral beta-amyloidogenesis is governed by agent and host. *Science.* **313** (5794), 1781-1784, doi:10.1126/science.1131864, (2006).
33. Luk, K. C. *et al.* Pathological alpha-synuclein transmission initiates Parkinson-like neurodegeneration in nontransgenic mice. *Science.* **338** (6109), 949-953, doi:10.1126/science.1227157, (2012).

34. Clavaguera, F. *et al.* Transmission and spreading of tauopathy in transgenic mouse brain. *Nat Cell Biol.* **11** (7), 909-913, doi:10.1038/ncb1901, (2009).
35. Nonaka, T. *et al.* Prion-like Properties of Pathological TDP-43 Aggregates from Diseased Brains. *Cell Rep.* **4** (1), 124-134, doi:10.1016/j.celrep.2013.06.007, (2013).
36. Lundmark, K. *et al.* Transmissibility of systemic amyloidosis by a prion-like mechanism. *Proc Natl Acad Sci U S A.* **99** (10), 6979-6984, doi:10.1073/pnas.092205999, (2002).
37. Lai, C. H., Chou, C. Y., Ch'ang, L. Y., Liu, C. S., & Lin, W. Identification of novel human genes evolutionarily conserved in Caenorhabditis elegans by comparative proteomics. *Genome Res.* **10** (5), 703-713 (2000).
38. Xu, X., & Kim, S. K. The early bird catches the worm: new technologies for the Caenorhabditis elegans toolkit. *Nat Rev Genet.* **12** (11), 793-801, doi:10.1038/nrg3050, (2011).
39. Boulin, T., & Hobert, O. From genes to function: the C. elegans genetic toolbox. *Wiley Interdiscip Rev Dev Biol.* **1** (1), 114-137, doi:10.1002/wdev.1, (2012).
40. Nussbaum-Krammer, C. I., Park, K. W., Li, L., Melki, R., & Morimoto, R. I. Spreading of a prion domain from cell-to-cell by vesicular transport in Caenorhabditis elegans. *PLoS Genet.* **9** (3), e1003351, doi:10.1371/journal.pgen.1003351, (2013).
41. Chernoff, Y. O., Lindquist, S. L., Ono, B., Inge-Vechtomov, S. G., & Liebman, S. W. Role of the chaperone protein Hsp104 in propagation of the yeast prion-like factor [psi+]. *Science.* **268** (5212), 880-884, doi:10.1126/science.7754373, (1995).
42. Liu, J. J., & Lindquist, S. Oligopeptide-repeat expansions modulate 'protein-only' inheritance in yeast. *Nature.* **400** (6744), 573-576, doi:10.1038/23048, (1999).
43. Halfmann, R. *et al.* Prions are a common mechanism for phenotypic inheritance in wild yeasts. *Nature.* **482** (7385), 363-368, doi:10.1038/nature10875, (2012).
44. Tyedmers, J., Madariaga, M. L., & Lindquist, S. Prion switching in response to environmental stress. *PLoS Biol.* **6** (11), e294, doi:10.1371/journal.pbio.0060294, (2008).
45. Krammer, C. *et al.* The yeast Sup35NM domain propagates as a prion in mammalian cells. *Proc Natl Acad Sci U S A.* **106** (2), 462-467, doi:10.1073/pnas.0811571106, (2009).
46. Hofmann, J. P. *et al.* Cell-to-cell propagation of infectious cytosolic protein aggregates. *Proc Natl Acad Sci U S A.* **110** (15), 5951-5956, doi:10.1073/pnas.1217321110, (2013).
47. Stiernagle, T. Maintenance of C. elegans. *WormBook.* doi:10.1895/wormbook.1.101.1, (2006).
48. Berkowitz, L. A., Knight, A. L., Caldwell, G. A., & Caldwell, K. A. Generation of Stable Transgenic C. elegans Using Microinjection. *J. Vis. Exp.* **18** e833, doi:10.3791/833, (2008).
49. Evans, T. C. (ed.) Transformation and microinjection. *WormBook.* doi:10.1895/wormbook.1.108.1, (2006).
50. Shaham, S. (ed.) Methods in cell biology. *WormBook.* doi:10.1895/wormbook.1.49.1, (2006).
51. Kim, E., Sun, L., Gabel, C. V., & Fang-Yen, C. Long-term imaging of Caenorhabditis elegans using nanoparticle-mediated immobilization. *PLoS One.* **8** (1), e53419, doi:10.1371/journal.pone.0053419, (2013).
52. Fay, D. Genetic mapping and manipulation: Chapter 1-Introduction and basics. *WormBook.* doi:10.1895/wormbook.1.90.1, (2006).
53. Kamath, R. S., & Ahringer, J. Genome-wide RNAi screening in Caenorhabditis elegans. *Methods.* **30** (4), 313-321, doi:10.1016/S1046-2023(03)00050-1, (2003).
54. Rual, J. F. *et al.* Toward improving Caenorhabditis elegans phenome mapping with an ORFeome-based RNAi library. *Genome Res.* **14** (10B), 2162-2168, doi:10.1101/gr.2505604, (2004).
55. Shaner, N. C., Steinbach, P. A., & Tsien, R. Y. A guide to choosing fluorescent proteins. *Nat Methods.* **2** (12), 905-909, doi:10.1038/nmeth819, (2005).
56. Kern, A., Ackermann, B., Clement, A. M., Duerk, H., & Behl, C. HSF1-controlled and age-associated chaperone capacity in neurons and muscle cells of C. elegans. *PLoS One.* **5** (1), e8568, doi:10.1371/journal.pone.0008568, (2010).
57. Becker, J., Walter, W., Yan, W., & Craig, E. A. Functional interaction of cytosolic hsp70 and a DnaJ-related protein, Ydj1p, in protein translocation *in vivo*. *Mol Cell Biol.* **16** (8), 4378-4386, (1996).
58. Salvaterra, P. M., & McCaman, R. E. Choline acetyltransferase and acetylcholine levels in Drosophila melanogaster: a study using two temperature-sensitive mutants. *J Neurosci.* **5** (4), 903-910, (1985).
59. Goloubinoff, P., Mogk, A., Zvi, A. P., Tomoyasu, T., & Bukau, B. Sequential mechanism of solubilization and refolding of stable protein aggregates by a bichaperone network. *Proc Natl Acad Sci U S A.* **96** (24), 13732-13737, doi:10.1073/pnas.96.24.13732, (1999).
60. Schroder, H., Langer, T., Hartl, F. U., & Bukau, B. DnaK, DnaJ and GrpE form a cellular chaperone machinery capable of repairing heat-induced protein damage. *EMBO J.* **12** (11), 4137-4144, (1993).
61. Rampelt, H. *et al.* Metazoan Hsp70 machines use Hsp110 to power protein disaggregation. *EMBO J.* **31** (21), 4221-4235, doi:10.1038/emboj.2012.264, (2012).
62. Gupta, R. *et al.* Firefly luciferase mutants as sensors of proteome stress. *Nat Methods.* **8** (10), 879-884, doi:10.1038/nmeth.1697, (2011).
63. Gidalevitz, T., Ben-Zvi, A., Ho, K. H., Brignull, H. R., & Morimoto, R. I. Progressive disruption of cellular protein folding in models of polyglutamine diseases. *Science.* **311** (5766), 1471-1474, doi:10.1126/science.1124514, (2006).
64. Ben-Zvi, A., Miller, E. A., & Morimoto, R. I. Collapse of proteostasis represents an early molecular event in Caenorhabditis elegans aging. *Proc Natl Acad Sci U S A.* **106** (35), 14914-14919, doi:10.1073/pnas.0902882106, (2009).
65. Karady, I. *et al.* Using Caenorhabditis elegans as a model system to study protein homeostasis in a multicellular organism. *J Vis Exp.* (82), e50840, doi:10.3791/50840, (2013).
66. Gidalevitz, T., Krupinski, T., Garcia, S., & Morimoto, R. I. Destabilizing protein polymorphisms in the genetic background direct phenotypic expression of mutant SOD1 toxicity. *PLoS Genet.* **5** (3), e1000399, doi:10.1371/journal.pgen.1000399, (2009).
67. Morley, J. F., Brignull, H. R., Weyers, J. J., & Morimoto, R. I. The threshold for polyglutamine-expansion protein aggregation and cellular toxicity is dynamic and influenced by aging in Caenorhabditis elegans. *Proc Natl Acad Sci U S A.* **99** (16), 10417-10422, doi:10.1073/pnas.152161099, (2002).
68. Brignull, H. R., Moore, F. E., Tang, S. J., & Morimoto, R. I. Polyglutamine proteins at the pathogenic threshold display neuron-specific aggregation in a pan-neuronal Caenorhabditis elegans model. *J Neurosci.* **26** (29), 7597-7606, doi:10.1523/JNEUROSCI.0990-06.2006, (2006).
69. Mohri-Shiomi, A., & Garsin, D. A. Insulin signaling and the heat shock response modulate protein homeostasis in the Caenorhabditis elegans intestine during infection. *J Biol Chem.* **283** (1), 194-201, doi:10.1074/jbc.M707956200, (2008).

70. Libina, N., Berman, J. R., & Kenyon, C. Tissue-specific activities of C. elegans DAF-16 in the regulation of lifespan. *Cell.* **115** (4), 489-502, doi:10.1016/S0092-8674(03)00889-4, (2003).
71. Schatzl, H. M. *et al.* A hypothalamic neuronal cell line persistently infected with scrapie prions exhibits apoptosis. *J Virol.* **71** (11), 8821-8831, (1997).
72. Keith, S. A., Amrit, F. R., Ratnappan, R., & Ghazi, A. The C. elegans healthspan and stress-resistance assay toolkit. *Methods.* doi:10.1016/j.ymeth.2014.04.003, (2014).
73. Pierce-Shimomura, J. T. *et al.* Genetic analysis of crawling and swimming locomotory patterns in C. elegans. *Proc Natl Acad Sci U S A.* **105** (52), 20982-20987, doi:10.1073/pnas.0810359105, (2008).

